BUTTERWORTH HEINEMANN

Polymer Vol. 36 No. 11, pp. 2181–2187, 1995
Copyright © 1995 Elsevier Science Ltd
Printed in Great Britain. All rights reserved
0032-3861/95/$10.00 + 0.00

The ultra-drawing behaviour of ultra-high-molecular-weight polyethylene: comparison of the gel-like spherulite pressing method and the gel-casting method

Toshihiko Ohta*, Akihiko Takada and Tomoko Yamamura
Faculty of Human Life Science, Osaka City University, Sumiyoshi, Osaka 558, Japan

and Akiyoshi Kawaguchi† and Syozo Murakami
Institute for Chemical Research, Kyoto University, Uji, Kyoto 611, Japan
(Received 25 May 1994; revised 11 October 1994)

Ultra-drawing behaviour has been studied by comparison of the gel-like spherulite pressing method and the gel-casting method using two kinds of specimens prepared from 2.0 wt% solution of ultra-high-molecular-weight polyethylene. The only major difference between the specimens is the cooling rate of solution. The influence of chain entanglement density in an undrawn specimen on the increase in strength and modulus with ultra-drawing has been discussed. The higher chain entanglement density of the undrawn specimen is the reason for the slopes of strength and modulus *versus* draw ratio being steeper in the gel-casting method. However, it was found that the differences in the above slopes between the two methods could not be explained by the changes in crystalline orientation and crystalline size with ultra-drawing.

(Keywords: UHMW polyethylene; ultra-drawing; gel-like spherulite)

INTRODUCTION

Since high-performance polyethylene (HP-PE) fibre, exceeding carbon and aramid fibres in strength and modulus, was developed by fibrillar crystal growth[1,2] and a gel-spinning/casting method[3,4], the processing principles of both methods have been applied to flexible polymers other than PE. High-performance fibres of high-molecular-weight poly(vinyl alcohol) have consequently been developed[5–7]. In ultra-high-molecular-weight polyethylene (UHMW-PE), there has been good progress in new processing methods for obtaining high-performance materials, i.e. the gel-like spherulite pressing method (called GSP method for short)[8,9], single-crystal drawing[10,11], virgin-polymer drawing[12–14] and reactor powder[15]. All of these methods are characterized by ultra-drawing of undrawn materials having an ultra-high (or high) molecular weight, which are prepared with little or no entanglement between polymer chains[16]. Such UHMW-PE materials can be easily ultra-drawn in the range of draw ratios from 30 to 300, depending on the entanglement density of the polymer chain[17,18].

The GSP method is distinct from the other methods in that gel-like spherulites formed from a semi-dilute solution of UHMW-PE are used: chain entanglements are introduced between lamellae in the gel-like spherulite, but there are no, or fewer, chain connections between spherulites[8]. In a previous paper[18], no influence of entanglement density of polymer chains in solution on the increase in strength and modulus was observed in this method. This was considered to be due to the small difference of chain entanglement density between the two kinds of gel-like spherulites formed from 1 and 2 wt% solutions of UHMW-PE, which was caused by disentanglement between polymer chains during crystallization from solution. So, in this paper, the influence of chain entanglement density on the increase in strength and modulus by ultra-drawing of UHMW-PE was investigated by using gel-cast sheet and GSP sheet, the cooling rate of solution being the only major difference between the preparation conditions of both sheets. Furthermore, X-ray diffraction studies on the ultra-drawing process of both sheets were carried out.

EXPERIMENTAL

Preparation of specimens

The 2 wt% solution was prepared by heating dispersions of UHMW-PE ($M_v = 2.3 \times 10^6$, Hizex-240M) powder in decalin to 160°C and holding for 30 min. Some 0.5 wt% of antioxidant (di-t-butyl-*p*-cresol) for the polymer was mixed in the solution to stabilize the polymer. The gel-like spherulites[9] and the gel-casting material[3] were respectively prepared by cooling the solution at a rate of

* To whom correspondence should be addressed
† Present address: Department of Chemistry, Faculty of Science and Technology, Ritsumeikan University, Kusatsu, Shiga 525, Japan

about 1.5°C min^{-1} and 16.5°C min^{-1} in the temperature range from 120 to 60°C.

The GSP sheet and gel-cast sheet were respectively prepared by compressing the accumulated material[9] of gel-like spherulites and gel-casting material under a pressure of 50 kg cm^{-2} at room temperature, and subsequently drying both compressed materials under reduced pressure at room temperature to remove the decalin. Both sheets were about 0.5 mm thick and contained 3 to 4 wt% decaline. The GSP sheet and gel-cast sheet were called A2 and C2 respectively.

Ultra-drawing of specimens

The ultra-drawing of specimens was carried out using a tensile tester equipped with an air oven. First, undrawn specimens, 20 mm long and 10 mm wide, were drawn to a draw ratio (*DR*) of 10 to 40 at a drawing speed of 10 mm min^{-1} at 100°C. The predrawn tapes were redrawn to the various *DR* under the above drawing conditions. The drawing temperature of 100°C was adopted because of the fact that no increase of long period of either sheet was observed after heating at 100°C for 15 min. The drawing of specimens was carried out after preliminary heating at 100°C for 10 min. The draw ratio was given as the denier ratio of undrawn and drawn specimens, which agreed well with that determined from the ratio of marking distance before and after drawing.

Measurement of strength and modulus

Measurement of tensile strength was carried out with a tensile tester at a deformation rate of 50% min^{-1} at room temperature. In measuring the modulus of high-modulus specimens with a tensile tester, slight slippage in the chuck may cause a large observational error, especially in the case of short specimens. In this study, therefore, a dynamic modulus was measured at a frequency of 100 Hz at room temperature. A viscoelastic spectrometer (Iwamoto Seisakusho, VES-III) was used for measuring the dynamic modulus of the specimen. The dynamic and tensile moduli agreed with those for a gel-spun fibre of UHMW-PE.

Dynamic X-ray diffraction experiment during ultra-drawing

Dynamic X-ray diffraction patterns during hot drawing at 100°C of specimens were recorded as a time series by X-ray diffraction apparatus equipped with imaging plates. The range of *DR* in each pattern was determined by the X-ray exposure time of 10 s. The recorded patterns were displayed on a PC screen for taking a photograph and processed on-screen for analysing the crystalline orientation and crystalline size. The undrawn specimens were drawn to a *DR* of 10 to 20 and these predrawn tapes after neck deformation were redrawn to a total *DR* of about 80 at 100°C at a deformation rate of 212% min^{-1} in an air oven, set up in the X-ray diffraction apparatus. During drawing, the incident X-ray beam was kept normal to the surface of the specimen. The *DR* was determined from the ratio of marking distance on the specimen.

RESULTS AND DISCUSSION

Fine structure of the undrawn specimen

The WAXD and SAXS patterns of GSP sheet A2 and gel-cast sheet C2 are apparently identical, as shown in *Figure 1*, whose surfaces in the edge patterns are parallel to the horizontal axis. The through patterns of WAXD

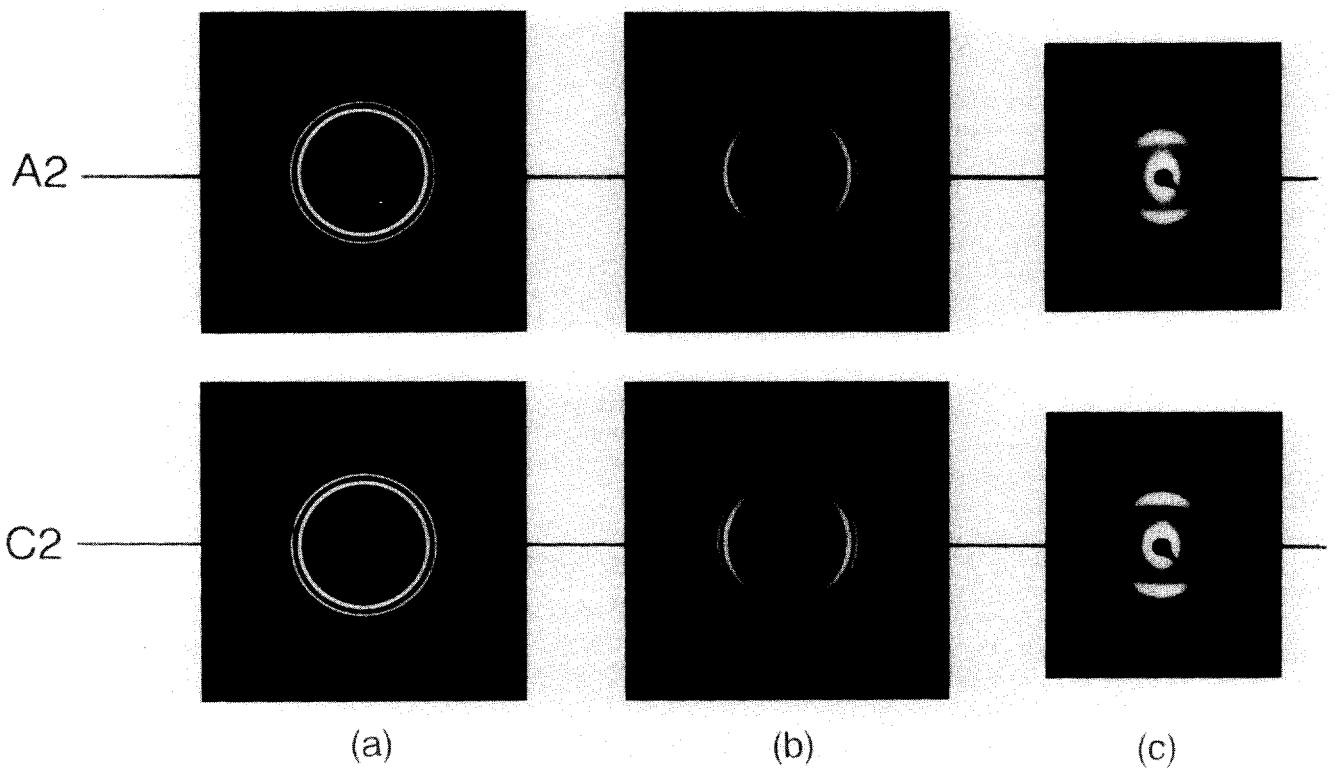

Figure 1 WAXD and SAXS patterns of a GSP sheet (A2) and a gel-cast sheet (C2), prepared from 2 wt% solution: (a) through pattern of WAXD; (b) edge pattern of WAXD; (c) edge pattern of SAXS

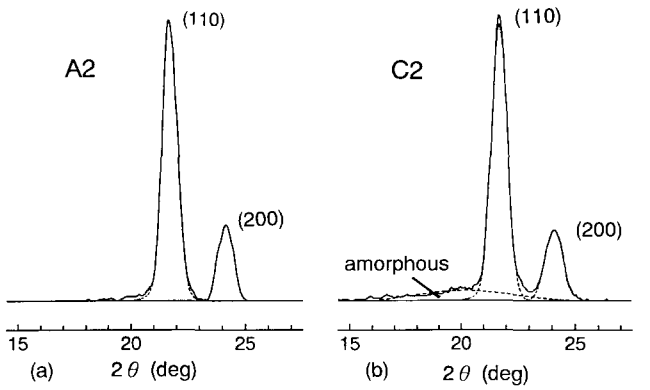

Figure 2 Equatorial WAXD profiles of (a) a GSP sheet (A2) and (b) a gel-cast sheet (C2), in which the incident X-ray beam is vertical to the surface of the sheet. The broken curves show the (1 1 0) and (2 0 0) diffractions

Table 1 Integral breadth in WAXD profile of the undrawn specimens, including the instrumental width

	Integral breadth (deg)	
Specimen	(1 1 0)	(2 0 0)
A2	0.87	0.79
C2	0.91	0.89

show strong diffraction rings from the (1 1 0) and (2 0 0) planes. The edge patterns of WAXD show preferential orientation of the (1 1 0) and (2 0 0) planes in the horizontal direction. These facts indicate that the lamellar surfaces in both A2 and C2 sheets are uniformly rotating around the vertical axis to both sheets and are oriented parallel to the sheet surfaces. In the edge patterns of SAXS of both sheets, strong interference from long-period structure can be observed in the vertical direction, which nearly corresponds to the lamellar thickness. This indicates that both sheets are composed of a multilayer structure formed by accumulation of lamellae, and each lamella is well packed. The long periods of the sheets were 126 Å for A2 and 105 Å for C2. This difference was considered to be caused by the difference in cooling rate of the solution. Equatorial WAXD profiles of both A2 and C2 sheets are shown in *Figure 2*, in which the incident X-ray beam is normal to the sheet surface. In the A2 sheet, both profiles of (1 1 0) and (2 0 0) diffractions were quite sharp, as shown in *Table 1*. This result shows that the crystalline size in both sheets is somewhat larger in the [2 0 0] direction than in the direction normal to the {1 1 0} planes, and that in both directions is larger in the A2 sheet than in the C2 sheet. Furthermore, an amorphous halo was observed in C2, but not in A2, as shown in *Figure 2*. This is compatible with the d.s.c. observation, as the heat of fusion was clearly larger for A2 (51 kcal g^{-1}) than for C2 (33 kcal g^{-1}). Moreover, no increase of long period of either sheet was observed after preliminary heating at 100°C for 15 min,

From these facts, it is found that the fine structures of both sheets are comparatively similar, and all of the above differences in the structural elements are based on the cooling rates of solutions in crystallizing polymers. Therefore, it is considered that the two sheets are adequate as comparable specimens for characterizing the ultra-drawing behaviour in the GSP method and elucidating the influence of chain entanglement density on the increase in strength and modulus by ultra-drawing of UHMW-PE.

Increase in strength and modulus by ultra-drawing

In the hot drawing at 100°C, clear neck deformation was observed for both A2 and C2 sheets. The neck draw ratio was different between both sheets, i.e. 10.0 for A2 and 17.5 for C2. The decreasing ratio of thickness at the neck was markedly larger than that of the width, i.e. 86% and 22% in A2, 92% and 28% in C2, respectively. Considering that both sheets are composed of a stack of lamellae, this necking phenomenon is inferred to be mainly due to the extension of a folded polymer chain in neck deformation. An apparently uniformly drawn tape was obtained at a *DR* of 35 to 40 in the case of C2, in relation to its neck *DR*.

Stress–strain curves at 100°C of the predrawn tapes with $DR = 40$ from both A2 and C2 sheets are shown in *Figure 3*. The maximum drawing stress (F) of C2 sheet (335 MPa) around the yield point is higher than that of A2 sheet (252 MPa), and the maximum draw ratio (λ_{max}) of C2 sheet (118) is somewhat lower than that of A2 sheet (136). It is obtained from this observation that λ_{max} is proportional to $F^{-1/2}$. This relation corresponds to that between λ_{max} and the contour length (L) of a chain segment between crosslinking points in the classic theory of rubber elasticity, as described in the previous paper[18]. This indicates that the ultra-drawing of both A2 and C2 sheets can be explained by the deformation of three-dimensional networks composed of chain entanglements, in spite of no (or fewer) connections between gel-like spherulites used for the A2 sheet. It is considered from this that pseudo-three-dimensional networks composed of chain entanglements are formed in the A2 sheet during compression of the accumulated material of gel-like spherulites including as much decalin as 90 wt%. The formation of networks in this way can be explained rationally by considering that the chain entanglements trapped in a gel-like spherulite are uniformly dispersed over the A2 sheet by the deformation of gel-like spherulites during their compression. More explicitly,

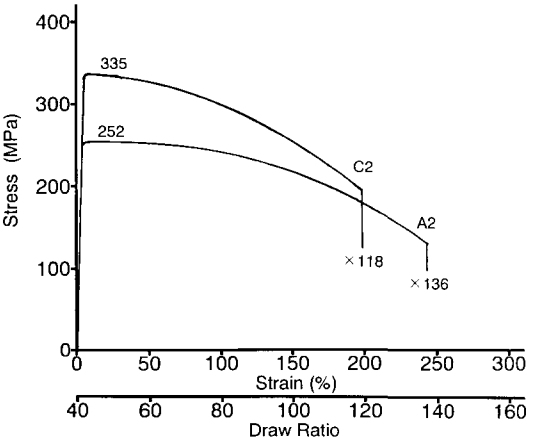

Figure 3 Stress–strain curves of predrawn tapes with $DR = 40$ from both sheets A2 and C2

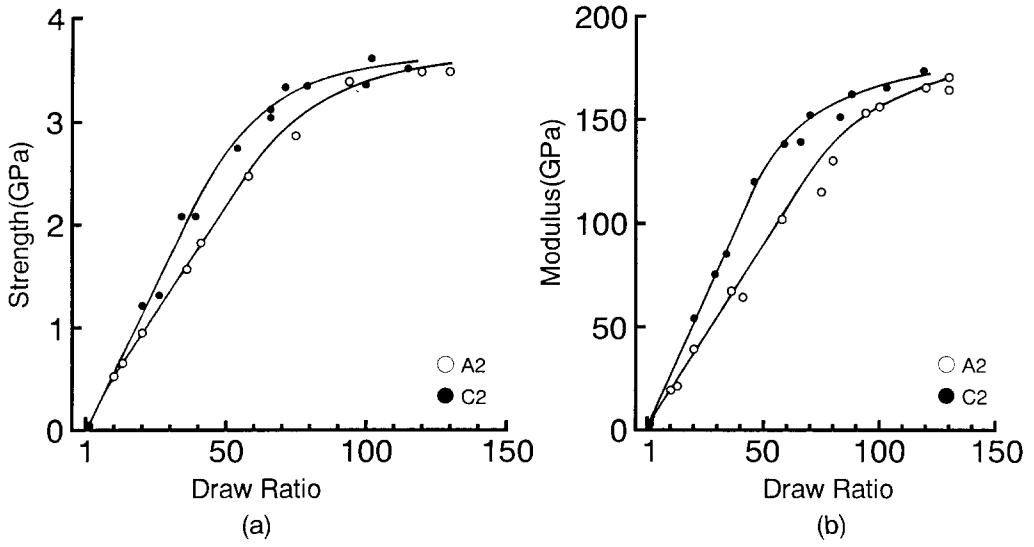

Figure 4 The increase in strength (a) and modulus (b) with ultra-drawing in both specimens A2 and C2

lamellae belonging to adjacent spherulites are mixed together during compression of the accumulated material of gel-like spherulites, and then the boundary surfaces of the spherulites disappear in the multilayer lamellar structure of the A2 sheet. This consideration is supported by the following facts: (1) The compressed sheets of 0.5 mm thickness prepared by compressing the dried spherulite powder under a pressure of 50 kg cm^{-2} at a temperature of 100 to 130°C could not be ultra-drawn at 100°C and their λ_{max} was around 10. The dried spherulite powder was prepared by only drying (not compressing) the accumulated material of gel-like spherulites used for A2 sheet under reduced pressure at room temperature. (2) The degree of crystalline orientation at the same *DR* is identical in both sheets A2 and C2 (see *Figures 5* and *6*), and clearly lower in the compressed sheet prepared from the dried spherulite powder than in the A2 sheet. From these facts, it is deduced that a pseudo-three-dimensional network composed of chain entanglements, similar to those in the C2 sheet, can also be formed in the A2 sheet. Therefore, considering that the chain entanglement density becomes lower in the A2 sheet than in the C2 sheet by disentanglement between polymer chains during crystallization from solution[18], it is deduced that the lower λ_{max} of C2 sheet is due to the higher chain entanglement density.

Kanamoto *et al.*[15] have reported that the drawability of a film of compressed UHMW-PE reactor powder was markedly improved by coextrusion of it. From the above information, it is difficult to consider that this improvement for second-stage drawing after coextrusion is caused by only the increase of adhesion and friction force between the boundary surfaces of reactor powder by coextrusion, because both forces can no longer play a connecting role between them at drawing temperatures of 120 to 135°C, which are considerably higher than the crystalline dispersion temperature (80°C) of polyethylene[19]. Hence, this phenomenon should be explained by the analogy to drawability of the GSP sheet, i.e. it is caused by more uniform transfer of drawing stress to each polymer chain through chain entanglement points, in comparison with that through adhesion and friction between the boundary surfaces of reactor powder, irrespective of the drawing temperature. The formation of pseudo-three-dimensional networks composed of chain entanglements in the coextruded film would proceed by dispersion of chain entanglements trapped in a particle of reactor powder over the coextruded film, similar to that in the GSP sheet, during coextrusion at 110°C of a film of compressed reactor powder. The value of λ_{max} (=77) in the drawn films of compressed UHMW-PE reactor powder[15] is considerably lower than that in GSP sheets A2. It is inferred from this that the chain entanglements are not so uniformly dispersed over the coextruded film as the GSP sheet A2.

The results on the increase in strength and modulus by ultra-drawing are shown in *Figure 4*. A linear relation of strength and modulus *versus DR* was obtained for $DR < 60$. The slopes of strength and modulus *versus DR* in the specimen C2 are clearly steeper than those of specimen A2, which are almost the same as those of gel-spun fibre from 2 wt% solution of UHMW-PE[3]. Considering the processing conditions, the fine structure and λ_{max} of both undrawn specimens, this difference in the above slopes should be due to the difference of chain entanglement density between both specimens, i.e. specimen C2 having a higher chain entanglement density shows steeper slopes of the increase in strength and modulus with ultra-drawing. This phenomenon can be understood as follows: In the specimen having a higher chain entanglement density, the drawing stress is more effectively transferred to each polymer chain through the chain entanglement points, and consequently the molecular orientation and fibrillar crystallization induced by chain extension are promoted more in the ultra-drawing process. On the other hand, the attained values of strength and modulus were almost the same in both specimens A2 and C2, but the slopes of strength and modulus *versus DR* in specimen C2 show a plateau at lower *DR*. It is inferred from this that the transition to the destruction process of fibrillar drawn structure occurs at an early stage of ultra-drawing in the specimen having a higher chain entanglement density.

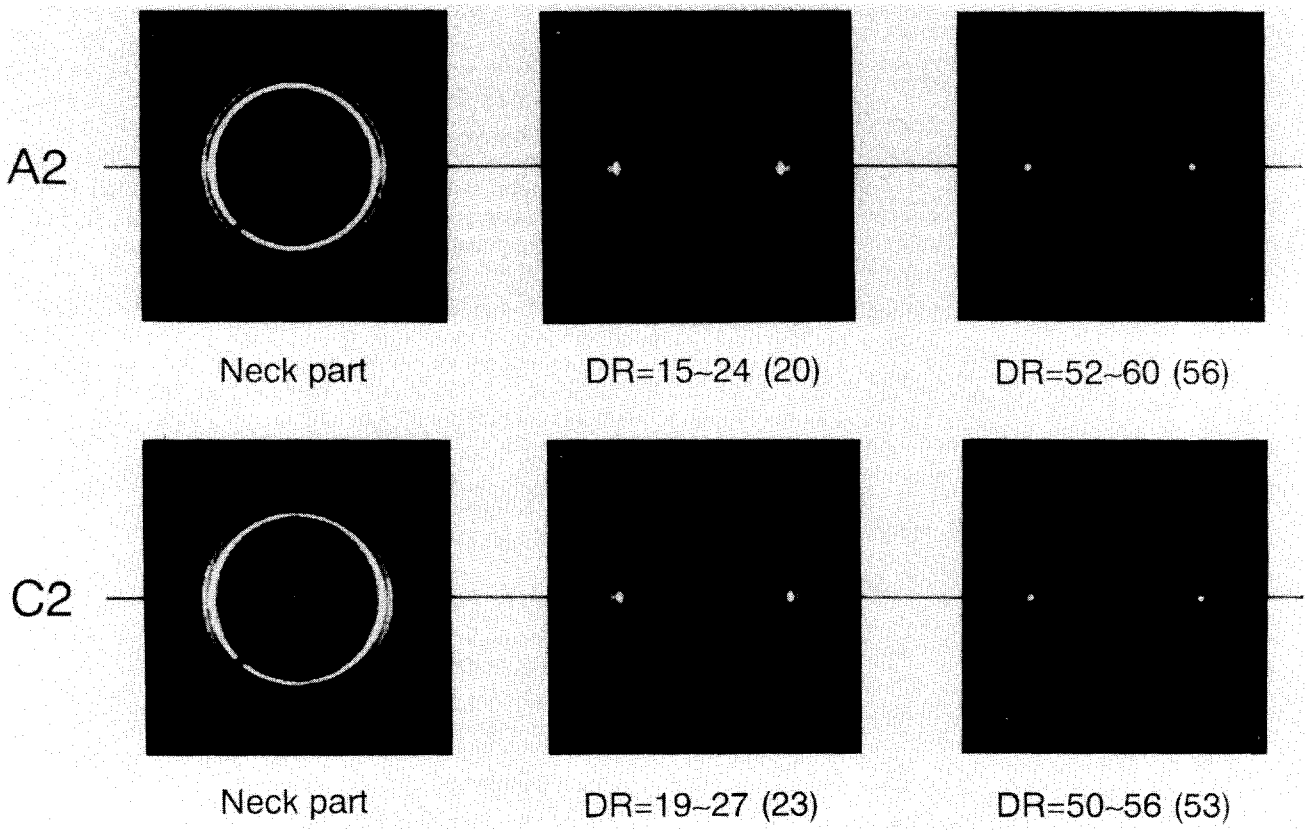

Figure 5 Dynamic X-ray diffraction patterns during ultra-drawing at 100°C of both specimens A2 and C2, taken using the imaging plate, in which the incident X-ray beam is normal to the surface of the specimen. The range of *DR* is determined by the X-ray exposure time of 10 s and is uncertain in the neck part

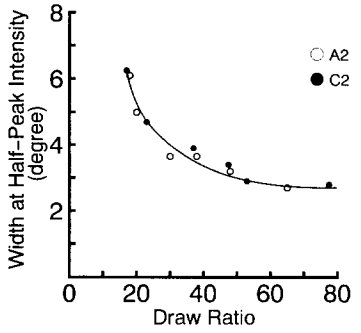

Figure 6 The width at half peak value of intensity profile along the Debye–Scherrer ring of (1 0 0) diffraction *versus DR*. The *DR* is the intermediate value in the range of *DR* in a dynamic X-ray diffraction pattern

Structural change during ultra-drawing

Dynamic X-ray diffraction patterns during ultra-drawing at 100°C of both specimens A2 and C2 were continuously taken using the imaging plates. The undrawn specimens were drawn to a *DR* of 10 to 20 and these predrawn tapes after neck deformation were redrawn to a *DR* of about 80, at 100°C at a deformation rate of 212% min^{-1} in an air oven. Representative patterns of both specimens A2 and C2 are shown in *Figure 5*, being taken with an X-ray exposure time of 10 s. In the neck part the arc-like (2 0 0) diffraction was observed. This means the fibrillar-like lamellae originated from spherulites rotate around the vertical axis to the specimen surface. In the *DR* of 15 to 24 and 19 to 27 in both specimens, no amorphous halo nor highly crystalline orientation were observed. In the *DR* of 50 to 60, the point-like (1 1 0) diffraction was observed and the (2 0 0) diffraction disappeared in both specimens. This indicates that the ultra-drawn tapes at a *DR* above 50 are remarkably close to a single crystal composed of mainly extended chains, since the *c* axis is parallel to the draw direction and the *a* axis is normal to the surface of the drawn tapes.

The changes of crystalline orientation and crystalline size during ultra-drawing at 100°C were pursued by analysing the intensity profile of dynamic X-ray diffraction patterns as shown in *Figure 5*. As a measure of the degree of *c*-axis orientation with respect to the draw direction, the observed widths at half peak value of intensity profiles along the Debye–Scherrer ring of (1 1 0) diffraction, including the instrumental width, are shown in *Figure 6*. The observed values of both specimens are depicted by a smoothly decreasing curve with increase of *DR*, in which the *DR* of horizontal axis is the intermediate value in the range of *DR* increased during taking a dynamic X-ray diffraction pattern. After neck deformation it shows 6.0°, which is considerably lower than that ($\simeq 10°$) of melt-spun nylon-6 (or polyester) fibre for tyre cord[20]. And it reaches to 2.7° by ultra-drawing beyond *DR* of 60, which seems to be the limit. This indicates that the *c*-axis orientation with respect to the draw direction proceeds remarkably during neck deformation corresponding to *DR* below 17 and gradually

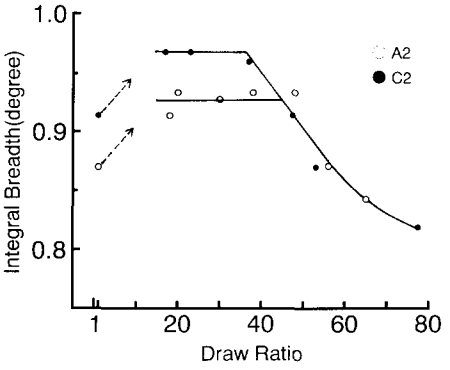

Figure 7 The integral breadth of equatorial intensity profile of (1 1 0) diffraction *versus DR*. The *DR* is the same as *Figure 6*

approaches the limit by further drawing to *DR* of 60. The changes of crystalline size in the direction normal to the {1 1 0} planes are shown in *Figure 7*, which are shown as the integral breadths of equatorial intensity profiles of (1 1 0) diffraction, including the instrumental width. The breadths of both specimens increase during neck deformation and clearly decrease after passing through a plateau with increase of *DR*. This behaviour has been observed in the drawing process of undrawn specimens composed of lamellar structure, for example, nylon-6 films cast from semi-dilute solution[21], and also observed in the ultra-drawing process of a gel-cast specimen of UHMW-PE[22]. However, a clear plateau could not be found in both observations. The detailed reasons for this difference are not clear at present, but it is inferred that a clear plateau in this study can be observed by carrying out dynamic WAXD experiments during hot drawing of the specimens. A range of *DR* showing a plateau is considered to correspond to the induction period until the increase of a diameter of microfibril starts, where microfibrils are formed during neck deformation as described later.

The *DR* at which the decrease in this breadth starts shows little difference between both specimens, but the decreasing rate of this breadth *versus DR* is almost the same between both specimens. The increase of the breadth implies the decrease of crystalline size during neck deformation. Thus, we see that the stacked lamellar structure of undrawn specimen should be destroyed and the fibrillar crystallization is concurrently induced by strain in the neck part of the specimen. The decrease of the breadth with further drawing signifies the growth of fibrillar crystals in the direction normal to the chain axis. Accordingly, it is found that the lateral growth rates of the crystallites are almost the same between both predrawn tapes.

Structure formed during neck deformation

In the meridional SAXS intensity curves of both predrawn tapes A2 and C2 with $DR = 20$, very weak interferences from the long-period structure of 165 Å were observed, which were clearly larger than those of undrawn specimens, i.e. 126 Å for A2 and 105 Å for C2. In both specimens, no interference was observed at $DR > 30$. These long periods did not change by further drawing after neck deformation, and were determined by drawing temperature as shown by Kawaguchi[23]. This indicates that the long-period structure exists even in predrawn tape at $DR < 20$ and disappears by further drawing at $DR > 30$. Therefore, it is deduced that two types of fibrillar structures are formed during neck deformation, as shown in the neck-deformation model of melt extrusion[24]: one is composed of folded-chain crystals (FCC) and the other of extended-chain crystals (ECC). The former would be newly re-formed with a breakage of lamellae, because its long period was determined by the drawing temperature irrespective of the long periods in the initial undrawn specimens. The latter was inferred to be induced by extension of the folded molecular chains of lamellar structure. In the further drawing process after neck deformation, the transformation from the FCC type of fibrillar structure to the ECC type was inferred to proceed by extending the folded chains, i.e. the growth of crystallites in the direction parallel to the chain axis, and eventually the fraction of the ECC type of fibrillar structure would approach 100%.

CONCLUDING REMARKS

A linear relation of strength and modulus *versus DR* was obtained for $DR < 60$. The slopes of strength and modulus *versus DR* were clearly steeper in the C2 specimen than in the A2 specimen. This difference was concluded to be due to the difference of chain entanglement density, by considering the fine structure and λ_{max} of both undrawn specimens. This phenomenon can be explained as follows: In the specimen having a higher chain entanglement density, the drawing stress is more effectively transferred to each polymer chain through the chain entanglement points, and consequently the molecular orientation and the fibrillar crystallization induced by chain extension are promoted more in the ultra-drawing process.

The structural change during neck deformation was most drastic in the ultra-drawing process. The degree of *c*-axis orientation with respect to the drawing direction drastically increased, and the crystalline size in the direction normal to the chain axis clearly decreased during neck deformation. Moreover, it was deduced that two types of fibrillar structures were formed during neck deformation: one is mainly composed of FCC and the other of ECC. In further drawing after neck deformation, the transformation from the FCC type of fibrillar structure to the ECC type was inferred to proceed, and eventually the fraction of ECC type would approach 100%.

However, no differences in the degree of *c*-axis orientation and the lateral growth rate of the ECC type of fibrillar crystal could be detected between both specimens C2 and A2. It was found from this that the effect of chain entanglement density on the increase of strength and modulus could not be explained in terms of these structural changes by ultra-drawing. Accordingly, the change in the content of folded molecular chains by ultra-drawing was investigated using *FT*i.r. spectroscopy, and its difference seemed to be detectable for both specimens. The details of this result will be presented in a forthcoming paper.

ACKNOWLEDGEMENT

This work was supported by a Grant-in-Aid (02452252) for Scientific Research from the Ministry of Education, Science and Culture, Japan.

REFERENCES

1 Zwijnenburg, A. Ph.D. Thesis, Groningen University, The Netherlands, 1978
2 Zwijnenburg, A. and Pennings, A. *Colloid Polym. Sci.* 1975, **253**, 452
3 Smith, P. and Lemstra, P. J. *Makromol. Chem.* 1979, **180**, 2983
4 Smith, P., Lemstra, P. J., Pijpers, J. P. L. and Kiel, A. M. *Colloid Polym. Sci.* 1981, **259**, 1070
5 Yoshikawa, W., Ohta, T., Okada, F. and Hayashi, M. Japan. Patent No. 63-028911, 1986
6 Hyon, S. H., Cha, W. I. and Ikada, Y. *Sen-i Gakkai Prepr.* 1987, 34
7 Yamaura, K., Tanigami, T., Hayashi, N., Kosuda, K., Okuda, S., Takemura, Y., Itoh, M. and Matsuzawa, S. *J. Polym. Sci.* 1990, **40**, 905
8 Ohta, T. and Okada, F. US Patent 4643865, 1987
9 Ohta, T., Okada, F., Hayashi, M. and Mihoichi, M. *Polymer* 1989, **30**, 2170
10 Furuhata, K., Yokokawa, T. and Miyasaka, K. *J. Polym. Sci., Polym. Phys. Edn.* 1984, **22**, 133
11 Kanamoto, T., Tsuruta, A., Tanaka, K., Takeda, M. and Porter, R. S. *Polym. J.* 1983, **15**, 327
12 Smith, P., Chanzy, H. D. and Rotzinger, B. P. *Polym. Commun.* 1985, **26**, 258
13 Chanzy, H. D., Rotzinger, B. P. and Smith, P. Patent WO-8703288
14 Smith, P., Chanzy, H. D. and Rotzinger, B. P. *J. Mater. Sci.* 1987, **22**, 523
15 Kanamoto, T., Ohama, T., Tanaka, K., Takeda, M. and Porter, R. S. *Polymer* 1987, **28**, 1517
16 Ohta, T. *New Mater. Japan. Prepr.* 1990, 201
17 Smith, P., Lemstra, P. J. and Booij, H. C. *J. Polym. Sci., Polym. Phys. Edn.* 1981, **19**, 877
18 Ohta, T., Wachi, T., Nagai, T., Takada, A., Ikeda, Y., Ohtsubo, T. and Kawaguchi, A. *Polymer* 1993, **34**, 4863
19 Takayanagi, M., Yoshino, M. and Hoashi, K. *Zairyou-Shiken* 1961, **10**, 418
20 Ohta, T., Mizukami, T. and Ogino, Y. *Sen-i Gakkaishi* 1991, **47**, 22; Ohta, T., 'Technical Information for Tire-cord', Toyobo Co. Ltd, 1970
21 Ohta, T., Yamashita, M., Yoshizaki, O. and Nagai, E. *Polym. Prepr. Japan* 1963, **12**, 117
22 van Aerle, N. A. J. M. Ph.D. Thesis, Eindhoven University of Technology, The Netherlands, 1989
23 Kawaguchi, A., Hirata, T., Nagasawa, T. and Kobayashi, K., International Conference on Mechanical Behavior of Polymers, 1971, Abstract, Vol. 2, p. 492
24 Peterlin, A. in 'Ultra-High Modulus Polymers' (Eds. A. Ciferri and I. M. Ward), Applied Science, London, 1979, Ch. 10